

Circ_0001971 regulates oral squamous cell carcinoma progression and chemosensitivity by targeting miR-194/miR-204 *in vitro* and *in vivo*

X. TAN¹, C. ZHOU², Y. LIANG^{1,3}, Y.-F. LAI¹, Y. LIANG¹

¹Department of Endodontics, School and Hospital of Stomatology, Guizhou Medical University/ Guizhou Medical University Affiliated Stomatological Hospital, Guiyang, Guizhou, China

²Peking University School and Hospital of Stomatology Second Clinic Center, Beijing, China

³Department of Stomatology, Guizhou Provincial People's Hospital, Guiyang, China

Abstract. – **OBJECTIVE:** Circular RNAs (circRNAs) play a wide role in human cancers, including oral squamous cell carcinoma (OSCC). The purpose of this study was to investigate the biological functions of circ_0001971 and associated mechanisms in OSCC.

MATERIALS AND METHODS: The expression of circ_0001971, miR-194, and miR-204 was detected by quantitative Real Time-Polymerase Chain Reaction (qRT-PCR). Cell proliferation and viability were assessed using cell counting kit-8 (CCK-8) assay. Cell migration and invasion were examined using the transwell assay. Cell apoptosis was monitored by flow cytometry assay. The protein levels of proliferation marker (CyclinD1), epithelial mesenchymal-transition (EMT) markers (E-cadherin (E-cad) and N-cadherin (N-cad)) and apoptosis markers (Cleaved-caspase-3 (Cleaved-cas-3) and Cleaved-caspase-9 (Cleaved-cas-9)) were measured by Western blot. The relationship between circ_0001971 and miR-194 or miR-204 was predicted by online tool starBase and verified by the Dual-Luciferase reporter assay and RNA immunoprecipitation (RIP) assay. Tumor formation assay in nude mice was conducted to observe the role of circ_0001971 *in vivo*.

RESULTS: The expression of circ_0001971 was significantly increased in tumor tissues and cell lines. Circ_0001971 knockdown inhibited cell proliferation, migration, and invasion but promoted cisplatin (DDP) sensitivity and cell apoptosis. It was confirmed that miR-194 and miR-204 were targets of circ_0001971, and miR-194 inhibition or miR-204 inhibition reversed the effects of circ_0001971 knockdown in OSCC cells. Moreover, circ_0001971 knockdown impeded tumorigenesis and development *in vivo*.

CONCLUSIONS: Circ_0001971 regulates cell proliferation, migration, invasion, apoptosis, and chemosensitivity of OSCC by interacting

with miR-194 and miR-204 *in vitro* and *in vivo*. We provided a theoretical basis for the action mechanism of circ_0001971 on OSCC progression and chemosensitivity.

Key Words:

Circ_0001971, MiR-194, MiR-204, OSCC, Chemosensitivity.

Introduction

Oral squamous cell carcinoma (OSCC) is a common malignancy that occurs in the oral and maxillofacial regions¹. OSCC has developed into the 6th most common malignant cancers, and the number of OSCCs is increasing every year^{2,3}. Despite recent advances in surgery, radiotherapy and chemotherapy have been made⁴, the mortality rate of OSCC patients is still not optimistic (about 50% to 60%) due to high prognosis, recurrence, metastasis, and resistance to chemotherapy drugs within five years^{2,5,6}. Therefore, it is worth finding novel markers for OSCC and to discover the application of potential gene therapy in the treatment of OSCC.

Circular RNAs (circRNAs), produced by back-splicing of precursor mRNA, are covalently closed circular RNA molecules⁷. Compared with linear RNAs, circRNAs are highly conserved and stable because there are no 3' poly (A) tail and 5' ends⁸. With the development of sequencing technique and bioinformatics, an increasing number of circRNAs has been identified. CircRNAs are associated with the development and progression of kinds of malignancies⁹, including

OSCC. Besides, a low level of circ-PKD2 in OSCC was associated with significant migration and invasion, and reintroduction of circ-PKD2 inhibited proliferation, migration, and invasion but stimulated apoptosis¹⁰. Has_circ_0092125 was down-regulated in OSCC tissues and cells, which was linked to tumor growth, tumor-node-metastasis (TNM) stage, and lymph node metastasis¹¹. Has_circ_0109291 expressed with a higher level in OSCC tissues compared with adjacent non-tumor tissues, and circ_0109209 knockdown suppressed proliferation and invasion in OSCC cell lines¹². These data suggested that circRNAs played diverse roles in the progression of OSCC, acting not only as oncogenes but also tumor suppressors. Zhao et al¹³ obtained a series of differently expressed circRNAs in saliva from OSCC patients by microarray analysis and found that circ_0001971 was significantly up-regulated. Circ_0001971 was back-spliced by FAM126A. However, the potential role of circ_0001971 in the progression of OSCC has not yet been mentioned.

CircRNAs interacted with microRNAs (miRNAs) to regulate the expression of miRNAs at the post-transcriptional level by acting as competitive endogenous RNAs (ceRNAs)^{14,15}. MiRNAs, a cluster of small non-coding RNA molecules with 18-25 nucleotides in length¹⁶, have been reported to participate in numerous cancers. MiR-194 functioned with contradictoriness in different types of cancer, such as acting as a tumor promoter in nasopharyngeal cancer¹⁷ or acting as a tumor suppressor in pancreatic cancer¹⁸. Whereas miR-204 usually functioned as a tumor inhibitor in cancer^{19,20}. Although the function of miR-194 and miR-204 has been partially mentioned in OSCC, their action mechanism needs further exploration to enrich the understanding of their roles.

Here, circ_0001971 was measured in OSCC tissues and cell lines. The functional role of circ_0001971 was determined *in vitro* and *in vivo*. Besides, the putative targets of circ_0001971 were identified to enrich the regulatory mechanism of circ_0001971 in OSCC. The objective of this research was to establish a promising biomarker for the treatment of OSCC.

Materials and Methods

Tissues Collection

OSCC tumor tissues (n=50) and adjacent non-tumor tissues (n=50) were collected from the

Guizhou Medical University School of Stomatology. These tumor tissues were classified into 2 groups according to TNM stage (I+II group and III+IV group). Prior to surgery, each patient had signed informed consent. All tissues were immediately treated with liquid nitrogen and next stored at a -80°C refrigerator. This research was authorized by the Ethics Committee of Guizhou Medical University School of Stomatology.

Cell Lines

OSCC cell lines (CAL-27 and SCC9) and human oral keratinocytes (HOK) were obtained from BeNa Culture Collection (Suzhou, China). SCC9 cells were maintained in 90% Roswell Park Memorial Institute-1640 (RPMI-1640; Sigma-Aldrich, St. Louis, MO, USA) containing 10% fetal bovine serum (FBS; Sigma-Aldrich). CAL-27 and HOK cells were cultured in 90% Dulbecco's Modified Eagle's Medium (DMEM; Sigma-Aldrich) containing 10% FBS (Sigma-Aldrich). All cells were maintained at 37°C conditions containing 5% CO₂.

Quantitative Real Time-Polymerase Chain Reaction (qRT-PCR)

Total RNA was isolated using TRIzol reagent (Invitrogen, Carlsbad, CA, USA) following the manufacturer's instruction. For circ_0001971, reverse transcription was performed using the Superscript III first-strand synthesis system (Life Technologies, Carlsbad, CA, USA). For miR-194 and miR-204, reverse transcription was performed using Mir-X miRNA First-Strand Synthesis Kit (Clontech, Mountain View, CA, USA). Next, an amplification reaction was conducted using SYBR Master Mix (Invitrogen, Carlsbad, CA, USA) on ABI 7500 Thermocycler (Applied Biosystems; Foster City, CA, USA). Relative expression was calculated using the 2^{-ΔΔCt} method and normalized by glyceraldehyde 3-phosphate dehydrogenase (GAPDH), 18S rRNA or U6 RNA. The sequences of primers were listed as follows: circ_0001971, forward 5'-GTG-GACCTCCTCCTCAAAGGG-3', and reverse 5'-AGCTGGTGACAGACAGGTTCT-3'; FAM126A, forward 5'-TGCAGTAACCAGCATGTCAA-3', and reverse 5'-CTAGACGCAGCCCTGGAATA-3'; miR-194, forward 5'-ATGGACCTGGGGCCAGCGAAG-3', and reverse 5'-TCTGGCCTGGGAGCGTCG-3'; miR-204, forward 5'-GCGGCGCAAAGAATTCTCCT-3', and reverse 5'-GTGCAGGGTCCGAGGT-3'; GAPDH, forward 5'-ATTCCACCCATGGCAAATTC-3',

and reverse 5'-TGGGATTTCCATTGATGA-CAAG-3'; U6, forward 5'-CTCGCTTCGGCAG-CAGCACATATA-3' and reverse 5'-AAATATG-GAACGCTTCACGA-3'; 18S, forward 5'-GTA-ACCCGTTGAACCCATT-3' and reverse 5'-CCATCCAATCGGTAGTAGCG-3'.

Cell Transfection

Lentiviral vector of circ_0001971 (lenti-short hairpin sh-circ) and its negative control (sh-NC) were obtained from Genechem (Shanghai, China) for stable circ_0001971 knockdown. MiR-194 mimics (miR-194), miR-204 mimics (miR-204), miR-194 inhibitor, miR-204 inhibitor, and their negative controls (miR-NC and anti-NC) were purchased from Ribobio (Guangzhou, China). All items were transfected into CAL-27 and SCC9 cells using Lipofectamine 2000 kit (Invitrogen, Carlsbad, CA, USA). Cells were harvested for subsequent analyses following 48-h incubation.

Cell Counting Kit-8 (CCK-8) Assay

Cell proliferation or viability was assessed using the Cell Counting Kit 8 (Beyotime, Shanghai, China). In brief, cells were seeded in 96-well plates (2×10^3 cells/well). After culturing for indicated time points (24 h, 48 h, and 72 h), cells were exposed to 10 μ L CCK-8 solution for another 2 h, and the OD value was measured at 450 nm in a spectrophotometer (Bio-Rad, Hercules, CA, USA).

Transwell Assay

CAL-27 and SCC9 cells with different transfection were harvested, resuspended in serum-free DMEM or RPMI-1640 containing 10% FBS and transferred into the upper 24-well transwell chambers (Corning Inc., Corning, NY, USA) for migration assay or chambers pre-coated with Matrigel (Corning Inc.) for invasion assay. Besides, DMEM or RPMI-1640 containing 10% FBS was added into the lower chambers. After culturing for 24 h, the migrated or invaded cells on the lower surface were fixed with 4% paraformaldehyde (PFA) and stained with methanol containing 0.1% crystal violet for another 15 min. Then, five randomly selected fields were taken to calculate cell amounts using an Olympus microscope (Olympus, Tokyo, Japan).

Western Blot

Total protein was extracted from tissues and cells using radioimmunoprecipitation (RIPA) lysis buffer (Beyotime). Total protein was quantified us-

ing a Bradford Protein Assay Kit (Beyotime) and then 20 μ g protein was separated by 10% sodium dodecyl sulfate-polyacrylamide gel electrophoresis (SDS-PAGE) and transferred onto polyvinylidene difluoride (PVDF) membranes (Bio-Rad, Hercules, CA, USA). After blocking for 1 h with 5% non-fat milk, the membranes were incubated with primary antibodies against CylinD1 (1:200; Cat. No. ab16663; Abcam, Cambridge, MA, USA), E-cadherin (E-cad) (1:10000; Cat. No. ab40772), N-cadherin (N-cad) (1:10000; Cat. No. ab76011), Cleaved-caspase-3 (Cleaved-cas-3) (1:500; Cat. No. ab32042), Cleaved-caspase-9 (Cleaved-cas-9) (1:500; Cat. No. ab2324) and GAPDH (1:2,000; Cat. No. ab9485) overnight at 4°C. Next, the membranes were incubated with horseradish peroxidase (HRP)-conjugated secondary antibodies (1:5000; Cat. No. ab205718; Abcam, Cambridge, MA, USA) for 2 h. Protein blots were visualized using the enhanced chemiluminescence reagent (ECL; Beyotime, Shanghai, China) on an imaging system (Bio-Rad, Hercules, CA, USA).

IC50 Detection

CAL-27 and SCC9 cells were seeded into 96-well plates at a density of 3×10^3 cells/well and treated without DDP or with DDP at different concentrations (1.25, 2.5, 5, 10, 20 and 40 μ M). After maintaining for 48 h, CCK-8 assay was utilized to detect cell viability. Then, the survival curve at different concentrations according to cell viability was depicted to reflect the half-maximal inhibitory concentration (IC50) value.

Flow Cytometry Assay

Flow cytometry assay was conducted to monitor cell apoptosis using Annexin V- fluorescein isothiocyanate (FITC)/propidium iodide (PI) Apoptosis Detection Kit (Beyotime, Shanghai, China). Briefly, CAL-27 and SCC9 cells with different transfection at 6-well plates were processed with 0.25% trypsin and washed with pre-cooled phosphate-buffered saline (PBS). Whereafter, cells (1×10^5) were resuspended in 195 μ L Annexin V-FITC binding buffer. Next, cells were incubated with 5 μ L Annexin V-FITC and 10 μ L PI staining solution for 15 min at room temperature in the dark. Finally, the apoptotic cells were analyzed using flow cytometer (BD Biosciences, Franklin Lakes, NJ, USA).

Actinomycin D Treatment

To detect the stability of circ_0001971, 2 mg/mL Actinomycin D (Sigma-Aldrich) was added into

CAL-27 and SCC9 cells with different transfection for 12 h before RNA isolation. Then, the qRT-PCR analysis was carried out as described above.

Nuclear and Cytoplasmic Localization Analysis

RNAs in cytoplasm and nucleus were extracted with the Cytoplasmic and Nuclear RNA Purification Kit (Norgen Biotek, Thorold, Canada). Total RNA in each fraction was used for qRT-PCR analysis. 18S rRNA or U6 was acted as the internal reference of the cytoplasm or nucleus.

Bioinformatics Prediction and Dual-Luciferase Reporter Assay

The target miRNAs of circ_0001971 were predicted by the online bioinformatics tool starBase (<http://starbase.sysu.edu.cn>).

To verify the relationship between circ_0001971 and miR-194 or miR-204, Dual-Luciferase reporter assay was executed. In brief, circ_0001971 wild-type sequences containing the binding site with miR-194 or miR-204 and corresponding circ_0001971 mutant sequences were respectively amplified and cloned into the downstream of pmirGLO vectors (Promega, Madison, WI, USA), named as circ_0001971 WT and circ_0001971 MUT. Afterwards, circ_0001971 WT or circ_0001971 MUT and miR-194 or miR-204 were co-transfected into CAL-27 and SCC9 cells, miR-NC acting as a control. Dual-Luciferase assay system (Promega) was used to detect Luciferase activities at 48 h after transfection.

RNA Immunoprecipitation (RIP) Assay

Magna RNA-binding protein immunoprecipitation kit (Millipore, Billerica, MA, USA) was utilized to execute RIP assay according to the manufacturer's protocol. Briefly, CAL-27 and SCC9 cells were harvested and dealt with RNA lysis buffer. Then, cell lysate was incubated with RIP buffer containing magnetic beads coated with human Ago2 antibody and mouse IgG antibody (control). Subsequently, immunoprecipitated RNA was extracted, and qRT-PCR was performed as above mentioned to detect the level of circ_0001971 and miR-194 or miR-204.

Tumor Formation Assay In Vivo

Mice experiments were authorized by the Animal Care and Use Committee of Guizhou Medical University School of Stomatology. BALB/c nude mice (n=20; 6-week-old; female) were purchased from HFK Bioscience (Beijing, China)

and averagely divided into 4 groups. LN229 cells, with sh-circ or sh-NC transfection for stable circ_0001971 knockdown, were subcutaneously injected into the right flank of mice groin. Subsequently, the mice were administered for 7 days in the same condition. Afterwards, the mice in one group with sh-circ injection were treated with 3 μ M DDP, and the mice in one group with sh-NC injection were also treated with 3 μ M DDP. Next, the tumor volume was recorded every 7 days according to the formula: volume=length \times width² \times 0.5. 35 days later, all mice were euthanized, and the tumors were removed for weighting and other molecular investigations.

Statistical Analysis

SPSS 20.0 (IBM, Armonk, NY, USA) was used for data process. Data were exhibited as mean \pm standard deviation (SD). Differences were analyzed by Student's *t*-test between two groups or one-way analysis of variance (ANOVA) among multiple groups followed by Tukey's test. Survival curve of patients was generated by Kaplan-Meier plot and analyzed by log-rank test. Each experiment consisted of three independent repetitions. *p* < 0.05 was regarded as statistically significant.

Results

Circ_0001971 Was Enriched in OSCC tissues and Cell Lines and Associated with TNM Stage and Overall Survival

The analysis of qRT-PCR was performed to determine the expression of circ_0001971 in OSCC tissues and cell lines. The result showed that the expression of circ_0001971 was increased in tumor tissues (n=50) compared with normal tissues (n=50) (Figure 1A). Besides, the expression of circ_0001971 in the advanced TNM stage (III/IV) (n=33) was significantly higher than that in the early TNM stage (I/II) (n=17) (Figure 1B). In addition, the overall survival of OSCC patients was observed, and the result presented that high expression of circ_0001971 led to a weaker overall survival rate within five years relative to low expression of circ_0001971 (Figure 1C). Likewise, the expression of circ_0001971 in OSCC cell lines (CAL-27 and SCC9) was notably elevated compared with that in normal oral keratinocytes (HOK) (Figure 1D). These data showed that highly expressed circ_0001971 was

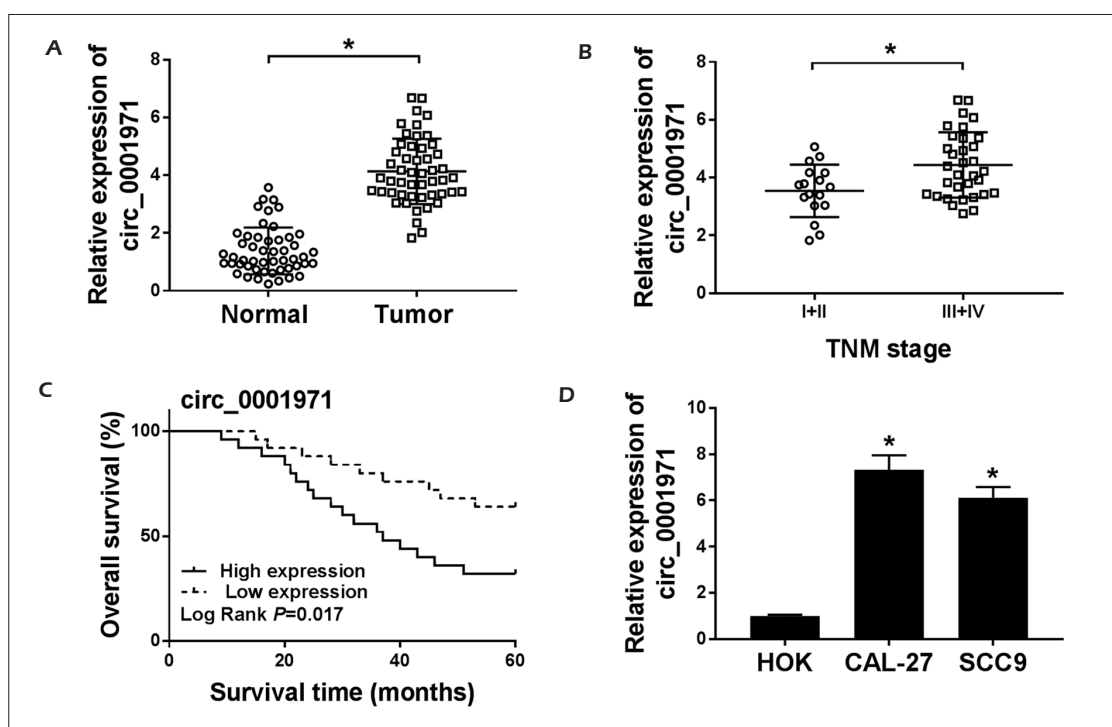


Figure 1. Circ_0001971 was up-regulated in OSCC tissues and cell lines. **A**, Expression of circ_0001971 in tumor tissues (n=50) and adjacent non-tumor tissues (n=50) was detected by qRT-PCR. **B**, Expression of circ_0001971 in the early TNM stage (I+II, n=17) and advanced TNM stage (circ_0001971+IV, n=33) was detected by qRT-PCR. **C**, Relationship between the overall survival of OSCC patients and circ_0001971 expression was analyzed according to the Kaplan-Meier plot and log-rank test. **D**, Expression of circ_0001971 in HOK, CAL-27, and SCC9 cell was detected by qRT-PCR. * $p < 0.05$.

monitored in OSCC tissues and cells, leading to poor prognosis.

Circ_0001971 Knockdown Inhibited Cell Proliferation, Migration, Invasion, and EMT in OSCC Cells

The endogenous level of circ_0001971 was knocked down in CAL-27 and SCC9 cells by transfecting with sh-circ to observe the role of circ_0001971. We found that the expression of circ_0001971 was significantly declined in CAL-27 and SCC9 cells with sh-circ transfection (Figure 2A). Then, CCK-8 assay revealed that circ_0001971 knockdown prominently suppressed the proliferation of CAL-27 and SCC9 (Figure 2B and 2C). Next, flow cytometry assay exhibited that the number of migrated and invaded cells was significantly reduced with circ_0001971 knockdown (Figure 2D). Additionally, the levels of proliferation-related marker and EMT markers were quantified by Western blot, and the analysis manifested that the expression of Cylind1 and N-cad was pronouncedly weakened with the downregulation of circ_0001971, while the expression of E-cad was reinforced (Fig-

ure 2E). These data suggested that circ_0001971 knockdown suppressed cell proliferation, migration, invasion, and EMT.

Circ_0001971 Knockdown Inhibited DDP Resistance but Induced Apoptosis in OSCC Cells

We determined the role of circ_0001971 on drug resistance and cell apoptosis. It was clearly concluded that cell viability was declined in a dose-dependent manner, and the cell viability in sh-circ group was always lower than that in sh-NC group. Besides, the IC50 of DDP in CAL-27 and SCC9 cells transfected with sh-circ was markedly lower than that in cells with sh-NC transfection (Figure 3A and 3B). Next, flow cytometry assay elucidated that the apoptosis rate was strongly elevated with circ_0001971 knockdown (Figure 3C). Additionally, the levels of apoptosis-related markers were investigated, and the result indicated that the expression of Cleaved-cas-3 and Cleaved-cas-9 was enhanced in CAL-27 and SCC9 cells introduced with sh-circ rather than sh-NC (Figure 3D and 3E). The data hinted that circ_0001971 knockdown atten-

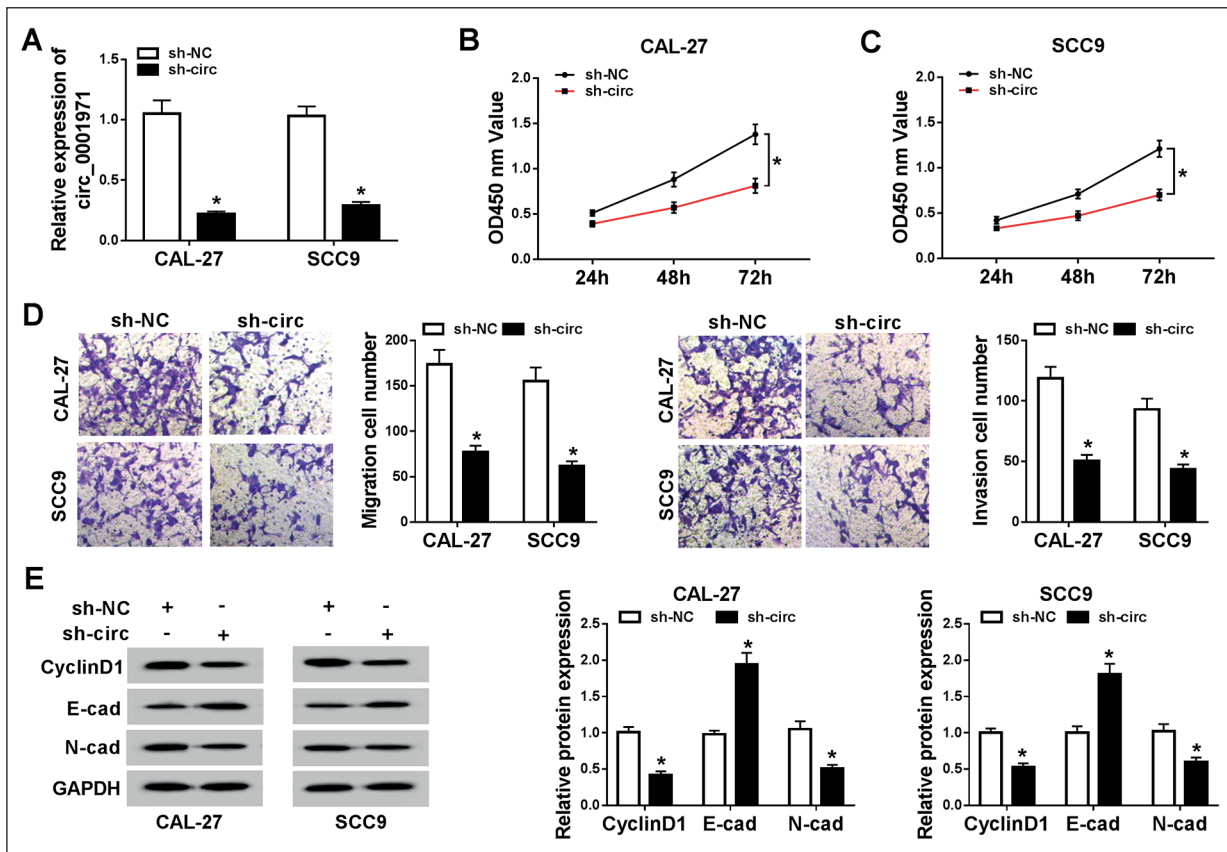


Figure 2. Circ_0001971 knockdown inhibited cell proliferation, migration, invasion, and EMT. **A**, Transfection efficiency was detected by qRT-PCR. **B, C**, Cell proliferation was assessed by CCK-8 assay. **D**, Cell migration and invasion were monitored by transwell assay (magnification 100 \times). **E**, Protein levels of CyclinD1, E-cad, and N-cad were quantified by Western blot. * $p < 0.05$.

uated DDP resistance and promoted the apoptosis rate in OSCC cells.

Circ_0001971 Directly Targeted MiR-194 and MiR-204

To explore the action mechanism of circ_0001971 in OSCC cells, the potential target miRNAs of circ_0001971 were identified. First, the stability of circ_0001971 was monitored, and we found that the RNA expression of circ_0001971 was invariably higher than FAM126A in CAL-27 and SCC9 cells treated with actinomycin D (Figure 4A and 4B), implying that circ_0001971 possessed higher stability than linear RNA FAM126A. Besides, the consequence of the qRT-PCR assay presented that circ_0001971 was mainly abounded in the cytoplasm compared with the cell nucleus (Figure 4C and 4D), supplying prerequisite for acting as a ceRNA of circ_0001971. Next, the underlying target miRNAs of circ_0001971 were predicted by bioinformatics tool. Among these miRNAs, miR-194 and

miR-204 were chosen for further experiments because their roles were previously mentioned in OSCC. The specific binding site between circ_0001971 and miR-194 or miR-204 was exhibited in Figure 4E. Next, the circ_0001971 mutant sequences were designed according to circ_0001971 wild-type sequences for Dual-Luciferase reporter assay, and the result showed that reintroduction of miR-194 or miR-204 strikingly dwindled the Luciferase activity in CAL-27 and SCC9 cells with circ_0001971 WT transfection relative to circ_0001971 MUT transfection (Figure 4F-4I). Moreover, RIP assay was performed, and higher levels of circ_0001971, miR-194, and miR-204 were observed in the anti-Ago2 group compared with that in the anti-IgG group (Figure 4J and 4K). The expression of miR-194 and miR-204 was notably weak in CAL-27 and SCC9 cells relative to that in HOK cells (Figure 4L and 4M), and the expression of miR-194 and miR-204 was substantially elevated with the downregulation of circ_0001971 (Figure 4N and 4O). These anal-

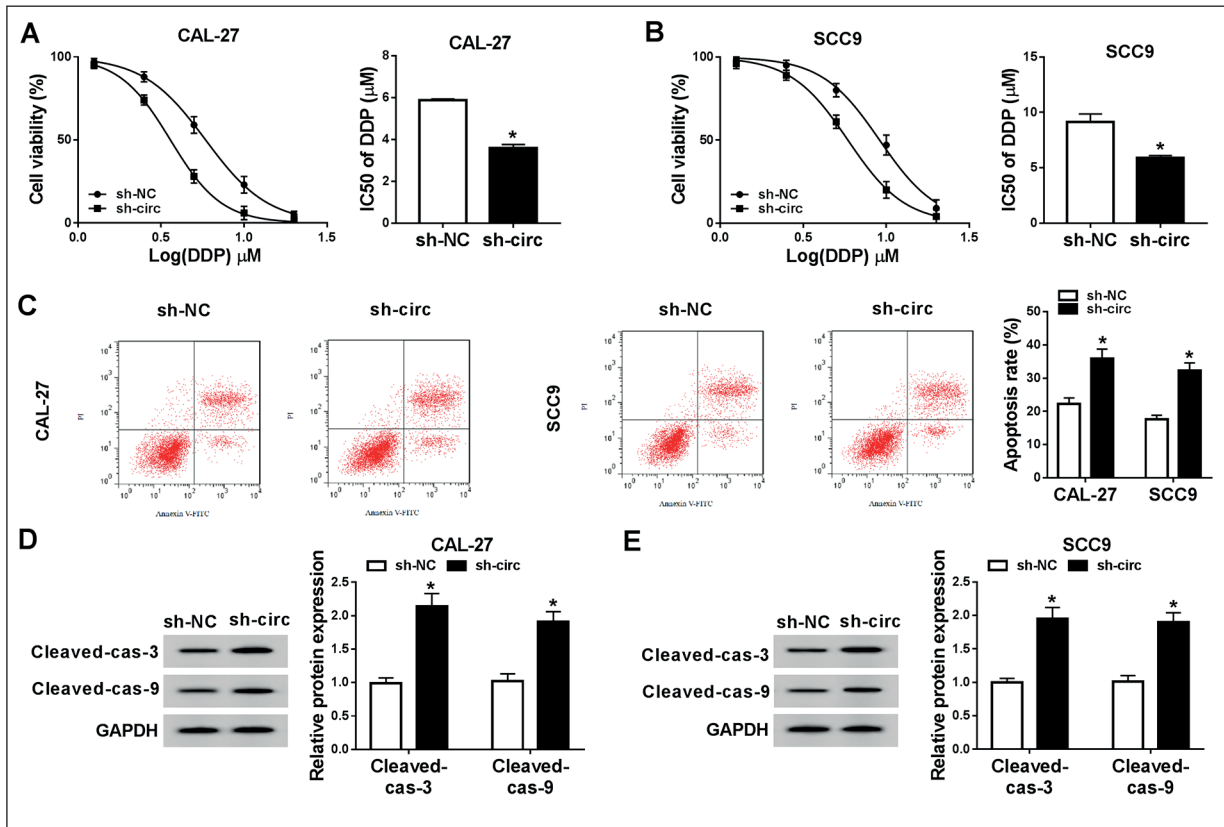


Figure 3. Circ_0001971 knockdown enhanced DDP sensitivity and cell apoptosis. **A, B,** Cell viability was detected by CCK-8 assay, and the IC₅₀ value was concluded according to cell viability. **C,** Cell apoptosis was determined by flow cytometry assay. **D, E,** Protein levels of Cleaved-cas-3 and Cleaved-cas-9 were quantified by Western blot. **p* < 0.05.

yses directed that miR-194 and miR-204 were directly targeted by circ_0001971.

Inhibition of MiR-194 or MiR-204 Reversed the Regulatory Effects of Circ_0001971 Knockdown in OSCC Cells

To ascertain whether circ_0001971 functioned by regulating miR-194 and miR-204, CAL-27 and SCC9 cells were transfected with sh-circ, sh-circ+anti-miR-194 and sh-circ+anti-miR-204, respectively. At first, the efficiency of miR-194 inhibition was examined, and we noticed that the expression of miR-194 or miR-204 was significantly decreased in CAL-27 and SCC9 cells with anti-miR-194 or anti-miR-204 transfection relative to anti-NC (Figure 5A and 5B). Of note, cell proliferation, inhibited by sh-circ, was recovered in CAL-27 and SCC9 cells transfected with sh-circ+anti-miR-194 or sh-circ+anti-miR-204 (Figure 5C and 5D). Likewise, cell migration and invasion, blocked by circ_0001971 knockdown alone, were re-

stored by miR-194 or miR-204 inhibition (Figure 5E and 5F). Additionally, the expression of CylinD1 and N-cad was reduced in cells transfected with sh-circ but reinforced in cells transfected with sh-circ+anti-miR-194 or sh-circ+anti-miR-204, while the expression of E-cad was opposite to N-cad expression in these transfection groups (Figure 5G-5I). Furthermore, the IC₅₀ of DDP, sequestered by circ_0001971 knockdown, was markedly rescued by miR-194 or miR-204 inhibition (Figure 5J). The apoptosis rate was promoted in CAL-27 and SCC9 cells transfected with sh-circ but markedly depleted in cells transfected with sh-circ+anti-miR-194 or sh-circ+anti-miR-204 (Figure 5K). In addition, the protein levels of Cleaved-cas-3 and Cleaved-cas-9, stimulated by circ_0001971 knockdown, were restrained by miR-194 or miR-204 inhibition (Figure 5L). Above data indicated that circ_0001971 knockdown exerted roles by increasing the expression of miR-194 and miR-204.

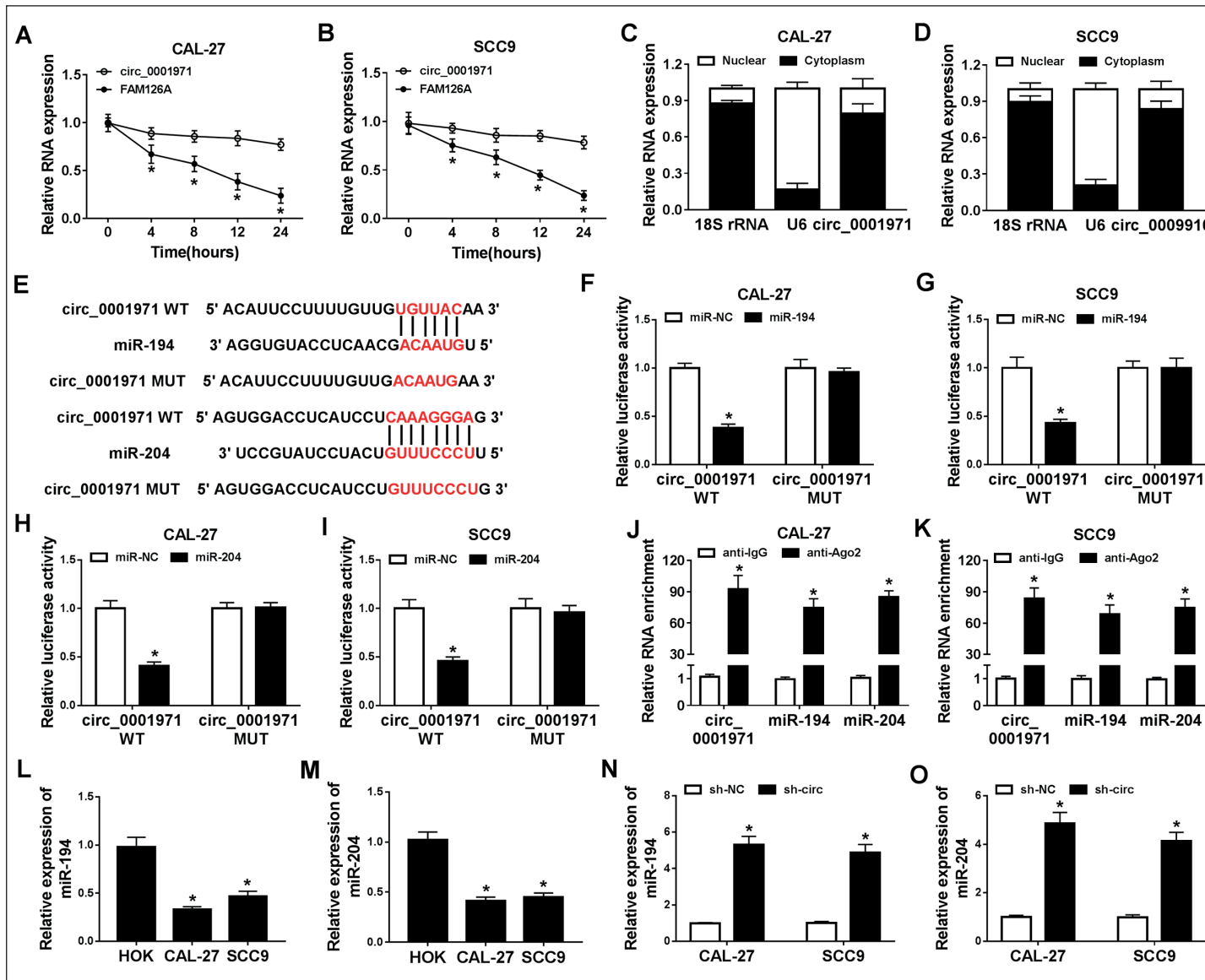


Figure 4. Circ_0001971 directly targeted miR-194 and miR-204. **A, B,** Stability of circ_0001971 was ascertained using actinomycin D. **C, D,** Enrichment of circ_0001971 in cytoplasm and nucleus was examined. **E,** Binding site between circ_0001971 and miR-194 or miR-204 was analyzed by online tool starBase. **F, G,** Interaction between circ_0001971 and miR-194 was verified by Dual-Luciferase reporter assay. **H, I,** Interaction between circ_0001971 and miR-204 was verified by Dual-Luciferase reporter assay. **J, K,** Relationship between circ_0001971 and miR-194 or miR-204 was further ensured by the RIP assay. **L, M,** Expression of miR-194 and miR-204 in HOK, CAL-27 and SCC9 cells was measured using qRT-PCR. **N, O,** Circ_0001971 knockdown enhanced the expression of miR-194 and miR-204. * $p < 0.05$.

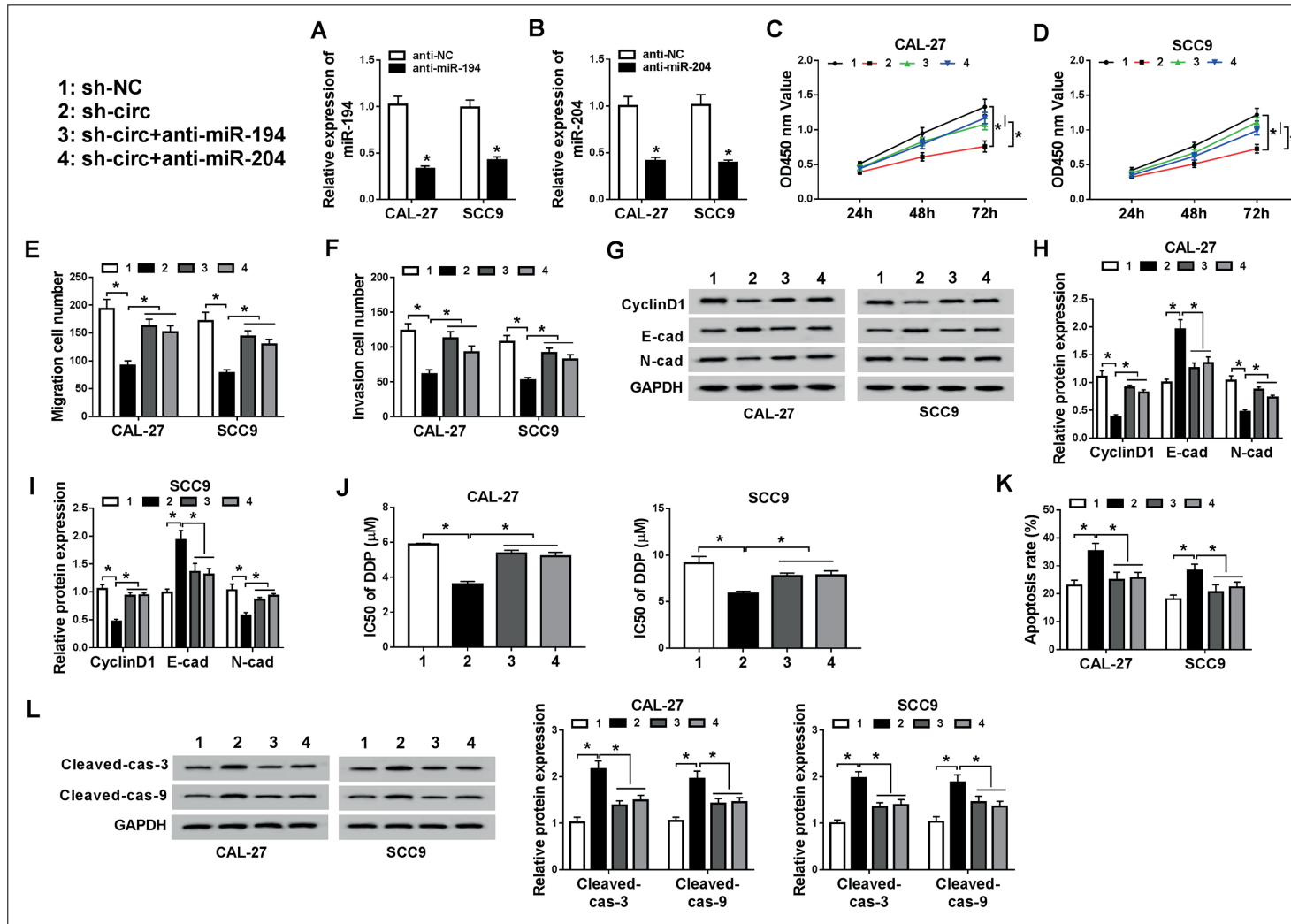


Figure 5. Inhibition of miR-194 or miR-204 reversed the role of circ_0001971 knockdown in CAL-27 and SCC9 cells. CAL-27 and SCC9 cells were introduced with sh-circ_0001971, sh-NC, sh-circ_0001971+anti-miR-194 or sh-circ_0001971+anti-miR-204. **A**, **B**, Transfection efficiency of miR-194 or miR-204 inhibition was detected by qRT-PCR. **C**, **D**, Cell proliferation was monitored by CCK-8 assay. **E**, **F**, Number of migrated and invaded cells was observed through the transwell assay. **G**, **H** and **I**, Protein levels of CyclinD1, E-cad, and N-cad were quantified by Western blot. **J**, The IC50 value was calculated based on cell viability detected by CCK-8 assay. **K**, Cell apoptosis was assessed by flow cytometry assay. **L**, Protein levels of Cleaved-cas-3 and Cleaved-cas-9 were quantified by Western blot. * $p < 0.05$.

Circ_0001971 Knockdown Impeded Tumorigenesis and Progression and Sensitized to DDP *In Vivo*

To further ascertain the role of circ_0001971 *in vivo*, the xenograft model in nude mice was established. As shown in Figure 6A and 6B, the tumor volume and weight in sh-circ group or sh-circ+DDP group were strikingly weaker than that in sh-NC group or sh-NC+DDP group. Besides, a more significant decrease of tumor volume and weight was observed in DDP-treated mice with sh-circ transfection relative to sh-NC transfection. Next, the qRT-PCR analysis showed that the expression of circ_0001971 in removed tumor tissues was

prominently reduced from the sh-circ group or sh-circ+DDP (Figure 6C), while the expression of miR-194 and miR-204 was markedly accelerated in the sh-circ group or sh-circ+DDP group (Figure 6D and 6E). Moreover, the expression of CyclinD1 and N-cad was suppressed in sh-circ group or sh-circ+DDP group, while the expression of E-cad was elevated in sh-circ group or sh-circ+DDP group compared with sh-NC group or sh-NC+DDP group (Figure 6F). The expression of Cleaved-cas-3 and Cleaved-cas-9 was enhanced in tumor tissues from sh-circ group or sh-circ+DDP group compared with that from sh-NC group or sh-NC+DDP group (Figure 6G).

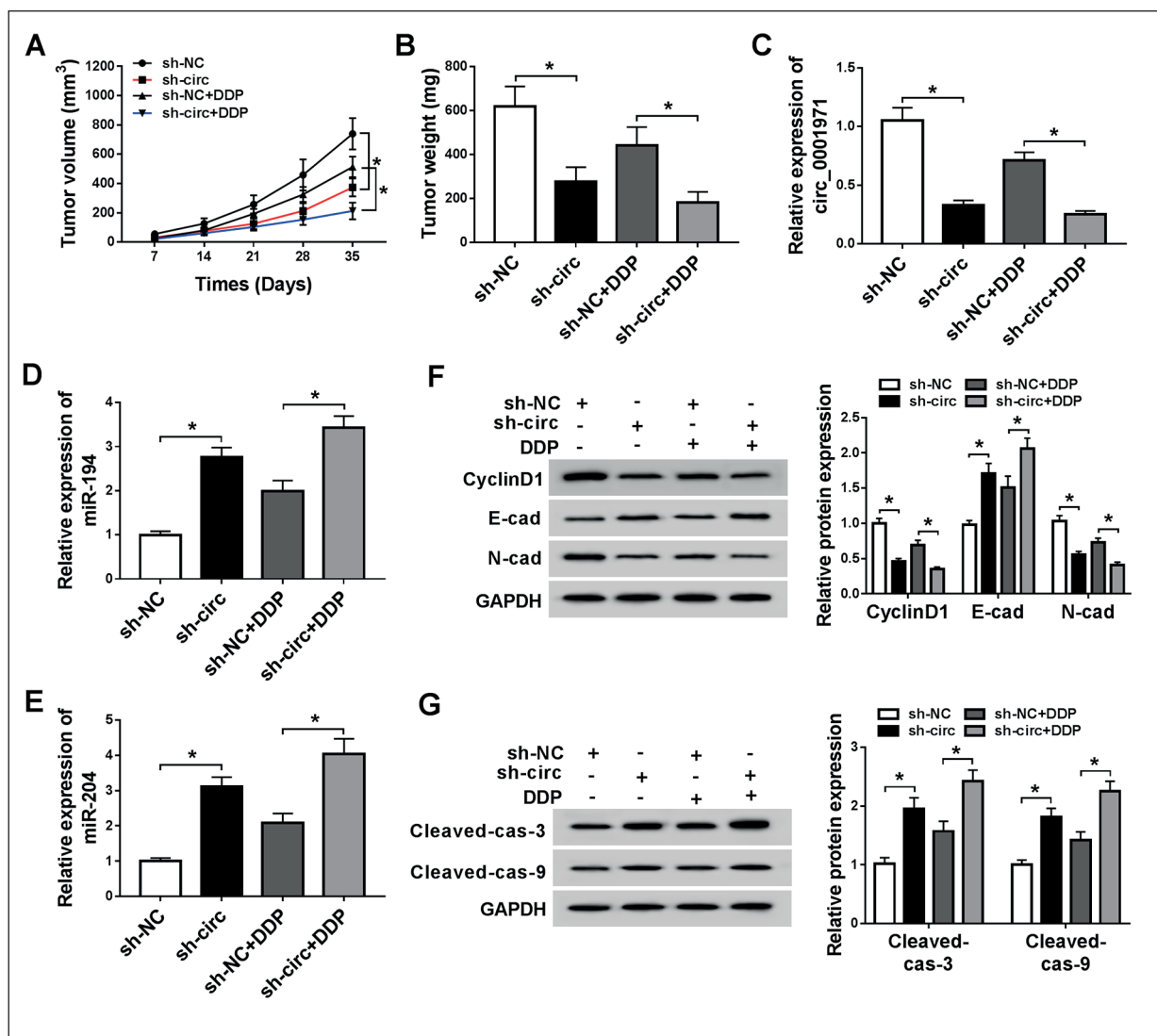


Figure 6. Circ_0001971 knockdown inhibited tumor growth and development *in vivo*. **A**, Tumor volume was recorded every 7 days. **B**, Tumors were weighed after 35 d-injection. **C**, **D** and **E**, Expression of circ_0001971, miR-194, and miR-204 in tumor tissues was detected by qRT-PCR. **F**, **G**, Protein levels of CyclinD1, E-cad, N-cad, Cleaved-cas-3, and Cleaved-cas-9 in tumors were quantified by Western blot. * $p < 0.05$.

Thus, we concluded that circ_0001971 knockdown strengthened the DDP sensitivity of OSCC, inhibited proliferation, migration, and invasion, but induced apoptosis *in vivo*.

Discussion

OSCC is the representative of head and neck squamous cell carcinoma, which has raised much public concern²¹. Understanding the mechanisms of OSCC progression and drug resistance is pivotal to develop more effective treatment strategies for OSCC. In this study, we noticed that circ_0001971 was richly expressed in OSCC tissues and cell lines, and high expression of circ_0001971 was associated with TNM stage and poor prognosis. Function analysis revealed that circ_0001971 knockdown attenuated cell proliferation, migration, invasion, EMT, and DDP resistance, but induced apoptosis *in vitro* and *in vivo*. Mechanism analysis concluded that miR-194 and miR-204 were targets of circ_0001971, and their inhibition could reverse the effects of circ_0001971 knockdown in OSCC cells.

Although dysregulation of circRNAs is implicated in various cancers, the specific role of circRNAs and associated mechanisms in OSCC are still limited. Notably, Zhao et al¹³ obtained a circRNA (circ_0001971) that was significantly up-regulated in the saliva of OSCC patients through microarray analysis, and its expression level was linked to the clinicopathological characteristics of OSCC patients. In accordance with this research, the expression of circ_0001971 in tumor tissues collected from 50 OSCC patients was notably elevated relative to matched non-tumor tissues. Besides, the expression of circ_0001971 was also enhanced in OSCC cell lines (CAL-27 and SCC9) relative to HOK cells. Furthermore, we conducted several molecular experiments *in vitro* to ensure the potential role of circ_0001971, and we observed that circ_0001971 knockdown inhibited malignant behaviors in CAL-27 and SCC9 cells, including proliferation, migration, invasion, EMT and DDP resistance. EMT is a developmental process that promotes the movement of otherwise adherent epithelial cells, and tumor cells may increase their aggressiveness by reactivating EMT programs²². EMT has been served as vital modulator of metastasis by inducing invasion or dissemination of tumor cells to distant organs²³. Additionally, numerous adverse prognostic reactions of OSCC, including

relapsed or recurrent disease, are associated with DDP resistance, and drug resistance is a major obstacle to cancer treatment failure²⁴. Our study presented that circ_0001971 knockdown weakened EMT and DDP resistance, suggesting that circ_0001971 was an oncogene in OSCC, and its knockdown helped to ameliorate the deterioration of OSCC.

CircRNAs generally function by acting as ceRNAs of downstream miRNAs. In our study, the expression of circ_0001971 was mostly enriched in cytoplasm other than the nucleus, which established the basis of circ_0001971 serving as a ceRNA. Hence, we speculated that circ_0001971 exerted its role in OSCC cells by mediating the expression of putative miRNAs. Eventually, miR-194 and miR-204 were chosen as targets of circ_0001971 for further analyses due to their roles were partly mentioned in OSCC in previous studies. MiR-194 was reported to be a tumor suppressor, and its overexpression blocked cell proliferation of OSCC by inactivating the PI3K-AKT-Fox3a pathway²⁵. Likewise, the expression of miR-204 was markedly weakened in oral cancer tissues^{26,27}, and miR-204-5p overexpression inhibited cell growth and metastasis in OSCC²⁸. These data indicated the tumor-suppressor features of miR-194 and miR-204 in OSCC. Our findings indicated that miR-194 and miR-204 were down-regulated in OSCC tissues and cells. Besides, miR-194 inhibition or miR-204 inhibition could reverse the effects of circ_0001971 knockdown in OSCC cells.

Conclusions

The expression of circ_0001971 was aberrantly elevated in OSCC tissues and cells. The functional role of circ_0001971 was first investigated in our study, and circ_0001971 knockdown alleviated cell proliferation, migration, and invasion, enhanced DDP sensitivity, and induced cell apoptosis *in vitro* and *in vivo*. Moreover, we first established the regulatory mechanism that circ_0001971 exerted its role in OSCC by targeting miR-194 and miR-204, providing a promising therapeutic target for OSCC.

Conflict of Interest

The Authors declare that they have no conflict of interests.

Funding

This work was approved by Doctoral Found of Guizhou Medical University (Grant No. Yuan Bo He J Zi [2015] 011th), Youth Science and Technology Talents Growth Project of Guizhou Education Department (Grant No. Qian Ji-ao He KY Zi[2018]195), and Found of Science and Technology Department of Guizhou Province (Grant No. Qian Ke He Ping Tai Ren Cai[2017]5718).

References

- 1) WONG RJ, KEEL SB, GLYNN RJ, VARVARES MA. Histological pattern of mandibular invasion by oral squamous cell carcinoma. *Laryngoscope* 2000; 110: 65-72.
- 2) KAMANGAR F, DORES GM, ANDERSON WF. Patterns of cancer incidence, mortality, and prevalence across five continents: defining priorities to reduce cancer disparities in different geographic regions of the world. *J Clin Oncol* 2006; 24: 2137-2150.
- 3) SASAHIRA T, KIRITA T, KUNIASU H. Update of molecular pathobiology in oral cancer: a review. *Int J Clin Oncol* 2014; 19: 431-436.
- 4) OMURA K. Current status of oral cancer treatment strategies: surgical treatments for oral squamous cell carcinoma. *Int J Clin Oncol* 2014; 19: 423-430.
- 5) BROCKLEHURST PR, BAKER SR, SPEIGHT PM. Oral cancer screening: what have we learnt and what is there still to achieve? *Future Oncol* 2010; 6: 299-304.
- 6) GASCHE JA, GOEL A. Epigenetic mechanisms in oral carcinogenesis. *Future Oncol* 2012; 8: 1407-1425.
- 7) ASHWAL-FLUSS R, MEYER M, PAMUDURTI NR, IVANOV A, BARTOK O, HANAN M, EVANTAL N, MEMCZAK S, RAJEWSKY N, KADENER S. CircRNA biogenesis competes with pre-mRNA splicing. *Mol Cell* 2014; 56: 55-66.
- 8) MEMCZAK S, JENS M, ELEFSINIOTI A, TORTI F, KRUEGER J, RYBAK A, MAIER L, MACKOWIAK SD, GREGERSEN LH, MUNSCHAUER M, LOEWER A, ZIEBOLD U, LANDTHALER M, KOCKS C, LE NOBLE F, RAJEWSKY N. Circular RNAs are a large class of animal RNAs with regulatory potency. *Nature* 2013; 495: 333-338.
- 9) KRISTENSEN LS, HANSEN TB, VENØ MT, KJEMS J. Circular RNAs in cancer: opportunities and challenges in the field. *Oncogene* 2018; 37: 555-565.
- 10) GAO L, ZHAO C, LI S, DOU Z, WANG Q, LIU J, REN W, ZHI K. Circ-PKD2 inhibits carcinogenesis via the miR-204-3p/APC2 axis in oral squamous cell carcinoma. *Mol Carcinog* 2019; 58: 1783-1794.
- 11) GAO L, WANG QB, ZHI Y, REN WH, LI SM, ZHAO CY, XING XM, DOU ZC, LIU JC, JIANG CM, ZHI KQ. Down-regulation of hsa_circ_0092125 is related to the occurrence and development of oral squamous cell carcinoma. *Int J Oral Maxillofac Surg* 2019 Aug 16. pii: S0901-5027(19)31265-2. doi: 10.1016/j.ijom.2019.07.014. [Epub ahead of print].
- 12) OUYANG SB, WANG J, ZHAO SY, ZHANG XH, LIAO L. CircRNA_0109291 regulates cell growth and migration in oral squamous cell carcinoma and its clinical significance. *Iran J Basic Med Sci* 2018; 21: 1186-1191.
- 13) ZHAO SY, WANG J, OUYANG SB, HUANG ZK, LIAO L. Salivary circular RNAs Hsa_Circ_0001874 and Hsa_Circ_0001971 as novel biomarkers for the diagnosis of oral squamous cell carcinoma. *Cell Physiol Biochem* 2018; 47: 2511-2521.
- 14) KULCHESKI FR, CHRISTOFF AP, MARGIS R. Circular RNAs are miRNA sponges and can be used as a new class of biomarker. *J Biotechnol* 2016; 238: 42-51.
- 15) VICENS O, WESTHOF E. Biogenesis of circular RNAs. *Cell* 2014; 159: 13-14.
- 16) MIN A, ZHU C, PENG S, RAJTHALA S, COSTEA DE, SAPPKOTA D. MicroRNAs as important players and biomarkers in oral carcinogenesis. *Biomed Res Int* 2015; 2015: 186904.
- 17) YIN W, SHI L, MAO Y. MiR-194 regulates nasopharyngeal carcinoma progression by modulating MAP3K3 expression. *FEBS Open Bio* 2019; 9: 43-52.
- 18) SUN Y, ZHU Q, YANG W, SHAN Y, YU Z, ZHANG Q, WU H. LncRNA H19/miR-194/PFTK1 axis modulates the cell proliferation and migration of pancreatic cancer. *J Cell Biochem* 2019; 120: 3874-3886.
- 19) SUN X, SU S, ZHANG G, ZHANG H, YU X. MiR-204 suppresses cell proliferation and promotes apoptosis in ovarian granulosa cells via targeting TPT1 in polycystic ovary syndrome. *Biochem Cell Biol* 2019; 97: 554-562.
- 20) LI N, GUO X, LIU L, WANG L, CHENG R. Molecular mechanism of miR-204 regulates proliferation, apoptosis and autophagy of cervical cancer cells by targeting ATF2. *Artif Cells Nanomed Biotechnol* 2019; 47: 2529-2535.
- 21) JEMAL A, SIEGEL R, XU J, WARD E. Cancer statistics, 2010. *CA Cancer J Clin* 2010; 60: 277-300.
- 22) AIELLO NM, KANG Y. Context-dependent EMT programs in cancer metastasis. *J Exp Med* 2019; 216: 1016-1026.
- 23) SANTAMARIA PG, MORENO-BUENO G, PORTILLO F, CANO A. EMT: present and future in clinical oncology. *Mol Oncol* 2017; 11: 718-738.
- 24) ZHOU X, REN Y, LIU A, JIN R, JIANG Q, HUANG Y, KONG L, WANG X, ZHANG L. WP1066 sensitizes oral squamous cell carcinoma cells to cisplatin by targeting STAT3/miR-21 axis. *Sci Rep* 2014; 4: 7461.
- 25) CHI H. MiR-194 regulated AGK and inhibited cell proliferation of oral squamous cell carcinoma by reducing PI3K-Akt-FoxO3a signaling. *Biomed Pharmacother* 2015; 71: 53-57.
- 26) TROIANO G, MASTRANGELO F, CAPONIO VCA, LAINO L, CIRILLO N, LO MUZIO L. Predictive prognostic value of tissue-based microRNA expression in oral squamous cell carcinoma: a systematic review and meta-analysis. *J Dent Res* 2018; 97: 759-766.
- 27) TSAI SC, HUANG SF, CHIANG JH, CHEN YF, HUANG CC, TSAI MH, TSAI FJ, KAO MC, YANG JS. The differential regulation of microRNAs is associated with oral cancer. *Oncol Rep* 2017; 38: 1613-1620.
- 28) WANG X, LI F, ZHOU X. MiR-204-5p regulates cell proliferation and metastasis through inhibiting CXCR4 expression in OSCC. *Biomed Pharmacother* 2016; 82: 202-207.